Expression of tau mRNA and soluble tau isoforms in affected and non-affected brain areas in Alzheimer's disease

A. Boutajangout, A. Boom, K. Leroy, J.P. Brion*

Laboratory of Histology, Neuropathology and Neuroanatomy, Université Libre de Bruxelles, School of Medicine, 808 route de Lennik, B-1070 Brussels, Belgium

Received 31 August 2004; accepted 6 September 2004

Available online 18 September 2004

Edited by Jesus Avila

Abstract In Alzheimer's disease (AD), selective expression of tau isoforms might underlie the susceptibility of different brain areas to develop neurofibrillary tangles and this pattern might change in the disease. In this study, we have analyzed in control subjects and in sporadic AD patients the pattern of expression of tau mRNA and tau proteins in areas unaffected (cerebellar cortex, white matter), moderately affected (occipital striate cortex, thalamus, caudate nucleus, and putamen) or strongly affected by neurofibrillary tangles (temporal and frontal associative cortex). After RT-PCR amplification, five products corresponding to the tau mRNAs containing exons 2 and 3, exon 2, without exons 2 or 3, with exon 10 and without exon 10 were identified. In control subjects, these five PCR products were present in all areas except in white matter, where transcripts with exons 2 or exons 2 and 3 were not identified. In AD patients, the same pattern of transcripts was observed in different areas, regardless of the presence of neurofibrillary lesions. After dephosphorylation of soluble tau proteins, the six tau isoforms were identified in the same areas by immunoblotting, including in the white matter, suggesting that most tau isoforms with exons 2 and 3 are transported along axons. The relative expression of 0N3R isoforms was higher in the temporal cortex than in the cerebellar cortex, both in control and AD subjects. The qualitative pattern of expression was identical in subjects with or without an APOE4 allele. Our results suggest that splicing regulation of the tau gene and the relative expression of tau isoforms are not significantly changed in sporadic cases of the disease, although differential expression of tau isoforms in temporal cortex might underlie this brain area susceptibility to neurofibrillary tangles formation.

Keywords: Alzheimer; tau mRNA; tau isoform; Neurofibrillary tangle; Cortex; Cerebellum; White matter

1. Introduction

Two neuropathological lesions characterize Alzheimer's disease (AD): senile plaques and neurofibrillary tangles (NFT). Senile plaques are composed of an extracellular core of Aβ amyloid surrounded by dystrophic neurites. NFT are constituted of bundles of abnormal filaments, called paired helical filaments (PHF), accumulating in neurons in selected brain areas. The PHF are composed of hyperphosphorylated forms of the microtubule-associated protein tau (PHF-tau proteins). Tau protein binds to microtubules and is involved in regulation of the stability of microtubules, axoplasmic transport and axonal differentiation. Six tau isoforms are expressed in adult human brain by alternative mRNA splicing from a single gene localized on chromosome 17 and containing 16 exons. These isoforms range from 352 to 441 amino acids in length and differ from each other by the presence or absence of three inserts encoded by exons 2, 3 and 10. The amino-terminal half of tau does not contain an insert (0N tau isoforms), or contains either an insert of 29 amino acids (encoded by exon 2, 1N tau isoforms), or 58 amino acids insert (encoded by exons 2 and 3, 2N tau isoforms). The carboxyl-terminal half of tau contains three or four semi-homologous repeats of 31 or 32 amino acids (encoded by exon 10, 3R or 4R tau isoforms) corresponding to microtubule-binding domains (for review, see [1,2]). These six tau isoforms have been identified in PHF extracted from AD brain tissue [3,4]. The spreading of NFT pathology in AD follows a relatively stereotyped sequence with limbic and neocortical associative areas being heavily affected at advanced stages, but with sparing of several brain regions (e.g., cerebellum, spinal cord) [5,6]. The detection of PHF-tau proteins in cortical areas in AD patients by biochemical methods follows a sequence comparable to that observed in neuropathological studies [7]. In other neurodegenerative diseases characterized by the presence of abnormal tau-positive fibrillary inclusions (tauopathies), the distribution of these cellular inclusions follows a different neuroanatomical pattern. These tau positive inclusions are composed of only selected tau isoforms, e.g., 3R tau isoforms in Pick's disease [1] or 4R tau isoforms in argyrophilic grain disease [8,9].

The pattern of expression of tau mRNAs and tau proteins in different human brain areas could underlie the propensity of these areas to develop or not neurofibrillary lesions and could explain the formation of tau aggregates formed of selected tau isoforms in different tauopathies. In addition, pathological changes in tau isoforms composition in selected brain areas could be instrumental in the induction of tau neurofibrillary lesions. For instance, some missense or silent mutations in exon 10 or in the intron following exon 10 (5′ splice site mutations), identified in familial forms of frontotemporal dementias and in other tauopathies [10,11], either increase the alternative splicing of exon 10, resulting in overproduction of 4 repeat tau mRNA and tau isoforms [12], or alter this splicing leading to an increase in three repeat tau isoforms [13]. The

* Corresponding author. Fax: +32-2-5556285.
E-mail address: jpbrion@ulb.ac.be (J.P. Brion).

0014-5793/$22.00
doi:10.1016/j.febslet.2004.09.011

splicing of the tau gene also shows a developmental regulation leading to developmental changes in tau isoforms expression [14,15]. However, only partial information is available on the distribution of tau transcripts and normal tau protein isoforms in the adult human brain. This study was thus aimed at investigating in parallel the distribution of tau mRNAs and tau protein isoforms in several neuroanatomically defined human brain areas, both in control subjects and in sporadic AD cases, in areas developing or not neurofibrillary lesions in the course of the disease.

2. Materials and methods

2.1. Human brain tissue

Human brains were obtained postmortem from five control individuals without neurological disease and from five patients with a diagnosis of probable or possible Alzheimer's disease (Table 1). These patients had no history of familial transmission of the disease. The mean age ($P = 0.11$) and postmortem intervals ($P = 0.55$) were not significantly different between the two groups (Student's t test). One hemisphere was cut into 1.5 cm thick slices in the frontal plane and dipped in liquid N2. These tissues were stored at −80 °C until use. The other hemisphere was fixed in 10% formalin. The neuropathological analysis showed the presence of numerous senile plaques and neurofibrillary tangles in patients with Alzheimer's disease and they were graded as stages V–VI (four cases) and III–IV (one case) for neurofibrillary degeneration according to the staging of [5].

2.2. RNA isolation

Samples of gray matter from the temporal cortex (inferior temporal gyrus), frontal cortex (inferior frontal gyrus), occipital cortex (gyrus lingula), caudate nucleus, putamen, thalamus, neocerebellar cortex and from the white matter (centrum semiovale) were dissected from the frozen tissues slices for RNA isolation. To assess the presence of NFT and amyloid deposits, small tissue blocks immediately adjacent to these samples were also dissected and fixed in formalin for immunohistochemical analysis (see below). For total RNA isolation, tissue samples (100 mg) were homogenized without prior thawing in RNase-free Teflon/glass homogenizers with 1 ml of TRIZOL Reagent (Invitrogen) and the homogenates were extracted by adding 0.2 ml of chloroform followed by centrifugation at 12 000 × g for 15 min at 4 °C. The upper aqueous phase was kept and 0.5 ml of isopropyl alcohol was added to precipitate RNA. After centrifugation, the pellet was washed with 1 ml of 75% (v/v) ethanol, dried and dissolved in RNase free water. Electrophoresis of RNA preparations on RNase free 1% agarose gel was used to assess RNA integrity (presence of non-degraded 18S and 28S ribosomal RNA). RNA concentration was measured by absorbance reading at 260 nm and the RNA samples were stored at −80 °C.

2.3. DNA isolation

Genomic DNA was extracted from tissue samples of the temporal cortex. 100 mg of tissue was homogenized in 0.5 ml of extraction buffer, using a glass-Teflon homogenizer and addition of 5 μl of ribonuclease A (RNAse A) (100 μg/ml). The homogenates were incubated for 1 h at 37 °C, then added with 10 μl of proteinase K (400 μg/ml). After an overnight incubation at 55 °C, samples were centrifuged at 13 000 × g for 10 min and 0.5 ml of DNAZOL (Gibco-BRL) was added to 0.5 ml of supernatants. After agitation for 30 min, samples were centrifuged at 13 000 × g for 10 min and 0.5 ml of absolute ethanol was added to 0.5 ml of supernatants, followed by centrifugation at 13 000 × g for 10 min. The pellets were washed in 0.2 ml of 70% (v/v) ethanol, dried and dissolved in TE. DNA concentration was measured by absorbance reading at 260 nm and the DNA samples were stored at −80 °C.

2.4. RT-PCR analysis

Analysis of tau mRNA expression by RT-PCR was performed by using the SuperScript One-Step RT-PCR kit with Platinium Taq System (Invitrogen). Single strand cDNA synthesis and PCR were performed in a single tube using specific tau primers and 3 μg of total RNA. For amplification of the 5′ half portion of tau mRNAs, the cDNAs were amplified by using the tau1 (forward) primer localized in exon 1 (5′-ATGGCTGAGCCCCGCCAGGAG-3′) and the tau4 (reverse) primer that spans exons 7 and 9 (5′-TGGAGGTTCACCAGAGCTGGG-3′). These tau primers allow for the simultaneous amplification of tau sequences with exons 2 and 3, exon 2 alone, or without these exons. Two primers were also designed to amplify the 3′ half portion of tau mRNAs: the tau3 primer that spans exons 7 and 9 (5′-CCCAGC TCTGGTGAACCTCCA-3′) and the tau2 primer localized in exon 13 (5′-TCACAAACCCTGCTTGGCCAG-3′). These tau primers allow for the simultaneous amplification of tau sequences with or without exon 10. The PCR was performed with a predenaturation step (55 °C for 30 min, then 94 °C for 2 min) followed by amplification steps carried out over 40 cycles (denaturation, 94 °C for 15 s; annealing, 60 °C for 30 s; extension, 72 °C for 60 s) and a final extension at 72 °C for 5 min. A RT-PCR for human β-actin (sense primer: 5′-CCTCGCCTTTGCCGATCC-3′; anti-sense primer: GGATCTTCATGAGGTAGTGAGTC-3′) was performed in parallel for normalization purposes. Products of RT-PCR were analysed by electrophoresis on 2% agarose gel in TAE and 12% polyacrylamide gel in TBE (0.0089 M Tris-base, 0.0089 M boric acid and 0.002 M EDTA, pH 8.0). The DNA bands were visualized by incubating gels with ethidium bromide for 10 min, and the gels were photographed using a digital camera.

2.5. PCR and restriction of amplified APOE gene

The APOE genotyping was performed using DNA samples extracted from control and AD cases brain tissue. The PCRs were carried out with the forward primer 5′-ACAGAATTCGCCCCG GCC TGGTACAC-3′ and the reverse primer 5′-TAAGC TTGGCACGGCTGTCCAAGGA-3′, as described [16]. Each reaction mixture was heated at 95 °C for 5 min for denaturation, and subjected to 30 cycles of amplification by primer annealing (60 °C for 1 min), extension (70 °C for 2 min), and denaturation (95 °C for 1 min). The PCR product of APOE gene amplification was digested with 5 units of *Hha*I for each reaction mixture (3 h at 37 °C). The digestion products were analysed by electrophoresis on 8% polyacrylamide gel in TBE.

2.6. Preparation of tau proteins

Brain tissue samples (from the same dissected blocks as those used for RNA isolation) from controls subjects and Alzheimer disease pa-

Table 1
Clinical and pathological data of human subjects used in this study

Cases	No.	Age	Sex	Postmortem delay	NFT staging	ApoE genotyping
Control	1	61	M	8	0	3/3
	2	65	M	4.5	0	2/3
	3	72	M	24	0	3/3
	4	77	F	48	0	3/4
	5	67	M	24	I–II	3/3
	Mean ± S.E.M.	68.4 ± 2.8		21.7 ± 7.7		
AD	6	72	F	24	V–VI	3/3
	7	70	F	21	V–VI	3/3
	8	71	M	24	III–IV	3/4
	9	91	F	5.5	V–VI	3/4
	10	84	M	7	V–VI	3/3
	Mean ± S.E.M.	77.6 ± 4.2		16.3 ± 4.1		

tients were homogenized in 4 vol of 0.1 mM 2-(*N*-morpholino)ethanesulfonic acid (MES), pH 6.5, added with protease inhibitors (leupeptin (1 μg/ml), pepstatin (1 μg/ml), soybean trypsin inhibitor (1 μg/ml), and aprotinin (1 μg/ml) (Roche). The homogenates were centrifuged at 300×*g* for 5 min at 4 °C and the supernatants used for analysis of total tau proteins. For analysis of soluble tau proteins, these supernatants were centrifuged at 20 000×*g* for 30 min at 4 °C and further centrifuged at 100 000×*g* for 1 h at 4 °C. These high-speed supernatants containing soluble tau proteins were further enriched in tau proteins by treatment with 2.5% (v/v) perchloric acid for 15 min on ice, followed by centrifugation for 20 min at 20 000×*g*. The final supernatants containing soluble tau protein were dialyzed against 50 mM Tris–HCl, pH 7.4, 1 mM dithiothreitol (DTT), and 0.1 mM phenylmethylsulfonyl fluoride (PMSF) overnight at 4 °C.

2.7. Dephosphorylation of tau

Human tau preparations in 50 mM Tris–HCl, pH 7.5, were dephosphorylated with 20 U/μl lambda phosphatase (New England Biolabs) for 3 h at 30 °C, as previously described [17]. The reaction was stopped by the addition of 5× (SDS–PAGE) sample buffer and heating for 5 min at 100 °C.

2.8. Western blotting

The products of dephosphorylation of tau proteins were separated by electrophoresis on 12% (w/v) polyacrylamide gels and proteins were transferred onto nitrocellulose membranes. For immunoblotting, the nitrocellulose sheets were blocked in semi-fat-dried milk (10% (w/v) in Tris-buffered saline; TBS) for 1 h and incubated with primary antibodies overnight, followed by anti-rabbit or anti-mouse immunoglobulins conjugated to alkaline phosphatase (Sigma). Finally, the membranes were incubated in developing buffer (0.1 M Tris–HCl, 0.1 M NaCl, and 0.05 M $MgCl_2$, pH 9.5) containing nitroblue tetrazolium and 5-bromo-4-chloro-3-indolyl phosphate. The densitometry analysis of immunoblots was performed using the NIH Image J program. Statistical analysis was performed using the Prism 4 software (Graphpad): differences among group means were calculated by one way analysis of variance and differences between individual groups were estimated by Bonferroni post hoc test for multiple comparisons.

2.9. Antibodies

The B19 antibody is a rabbit polyclonal antibody raised to adult bovine tau proteins [18]. This antibody reacts with all human and rodent tau isoforms in a phosphorylation-independent manner. BR10 is a polyclonal antibody raised to a synthetic peptide, specific for the insert 2 (encoded by exon 3) of tau [19]. The anti-Aβ amyloid antibody was purchased from Bio-Source.

2.10. Recombinant tau protein

Competent *E. coli* BL21-DE3 cells were transformed with a 2N4R pET30a tau plasmid and recombinant 2N4R tau protein was prepared as reported [20]. Induction of tau expression was performed by adding IPTG (0.5 mM final concentration) for 2 h at 37 °C. Bacteria were centrifuged for 15 min at 3300×*g*, the pellet was washed with 50 mM MES, pH 6.5, and homogenized in 50 mM MES, pH 6.5, 1 mM DTT, 1 mM PMSF, 1 mM EDTA, 10 mM NaF, and 20 mM sodium pyrophosphate by sonication on ice, followed by centrifugation at 20 000×*g* for 15 min at 4 °C. The supernatant was adjusted to 0.5 M NaCl, heated for 10 min, and centrifuged for 2 h at 50 000×*g*. The supernatant was added with ammonium sulfate to obtain a 45% concentration, mixed on ice for 1 h to precipitate proteins and centrifuged for 20 min at 30 000×*g*. After centrifugation, the pellet was dissolved in a small volume of dialysis buffer (50 mM MES, pH 6.5, 1 mM DTT, and 1 mM PMSF) and dialyzed overnight.

3. Results

3.1. Concentration of total RNA is similar in areas with or without NFT

The total RNA concentrations were not significantly different between control (159.0–283.0 μg RNA/g tissue) and AD subjects (148.5–263.7 μg RNA/g tissue) in all the investigated brain areas (two-way ANOVA, $P = 0.10$), a result consistent with previous reports, e.g. [21,22]. The immunohistochemical analysis of tissue blocks adjacent to those used for RNA isolation confirmed the presence of numerous NFT in the frontal and temporal cortex of AD patients (Fig. 1) and their absence in control subjects. In AD patients, a moderate number of NFT were also detected in thalamic nuclei and a few NFT were observed in the caudate nucleus and the putamen. NFT were not detected in the cerebellar cortex of both AD and control subjects.

3.2. RT-PCR amplifications of the 5′ domain of tau mRNAs identify the same products in affected and non-affected areas in control subjects and AD patients

The use of primers tau1 and tau4 predicted the amplification of three fragments corresponding to PCR products of 393 bp (0N tau mRNAs), 480 bp (1N tau mRNAs) and 567 bp (2N tau mRNAs).

Fig. 2 shows the typical results of RT-PCR amplifications from samples of the cerebellar cortex and from the temporal cortex in five control cases (Fig. 2A) and in five AD cases

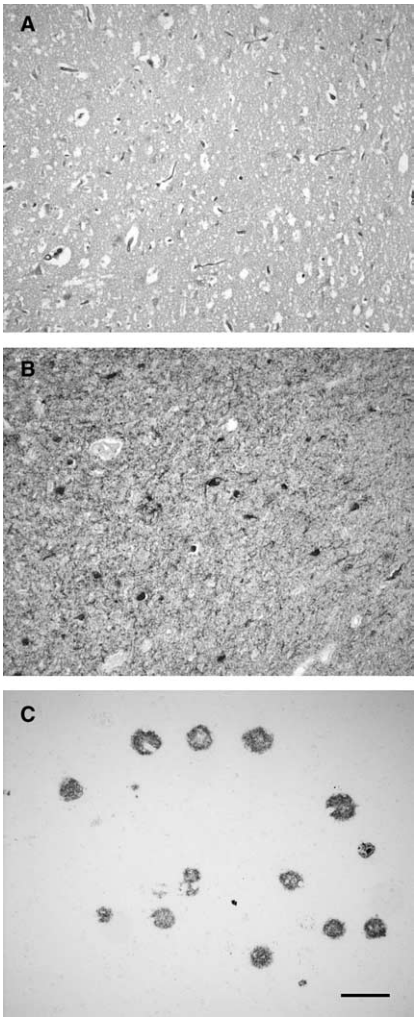

Fig. 1. Immunohistochemical labeling on tissue sections of the temporal cortex of (A) a control subject (Table 1, case no. 3), and (B and C) an AD patient (Table 1, case no. 10) with the B19 tau antibody (A and B) and the Aβ antibody (C). These tissue slides were adjacent to tissue blocks used for RNA extraction. Scale bar: 100 μm.

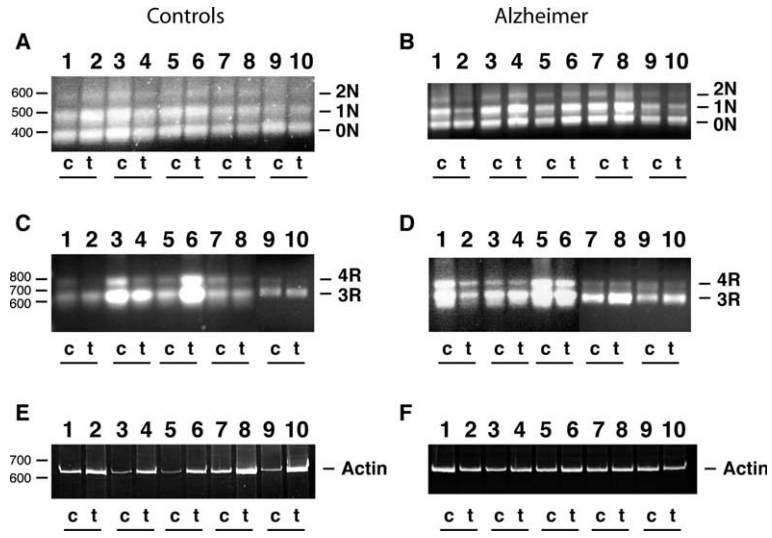

Fig. 2. Electrophoresis of RT-PCR amplification products of the 5′ domain of tau mRNAs (A and B), of the 3′ domain of tau mRNAs (C and D) and of actin mRNA (E and F) in the cerebellar cortex (c) and in the temporal cortex (t) in five control subjects (A, C, E, case nos. 1–5 in Table1) and in five AD patients (B, D, F, case nos. 6–10 in Table 1). The three PCR products in A and B correspond to tau mRNAs with exons 2 and 3 (2N), exon 2 (1N), or without these exons (0N). The two PCR products in C and D correspond to tau mRNAs with (4R) or without exon 10 (3R). Numbers on the left of lanes 1 indicate the position of calibration DNA fragments (in bp).

(Fig. 2B). The two PCR products of 393 and 480 bp were more abundant than the 567 bp PCR product, but the three PCR products were present in all samples. Fig. 3A and D shows that these three PCR products were also present in the frontal cortex (lanes 3), the occipital cortex (lanes 4), the caudate nucleus (lanes 5), the putamen (lanes 6) and in the thalamus (lanes 7), both in control subjects (Fig. 3A) and in AD patients (Fig. 3D). However in white matter, only the shortest 393 bp product was detected (lanes 8).

3.3. *RT-PCR amplifications of the 3′ domain of tau mRNAs identify the same products in affected and non-affected areas in control subjects and AD patients*

The use of primers tau3 and tau2 predicted the amplification of two fragments corresponding to PCR products of 686 bp (3R tau mRNAs) and 779 bp (4R tau mRNAs). Fig. 2C and D shows the typical results of RT-PCR amplifications from samples of the cerebellar cortex and from the temporal cortex in five control cases (Fig. 2C) and in five AD cases (Fig. 2D). The 686 bp PCR product was more abundant than the 779 bp PCR product, but they were both detected in all samples in control subjects and in AD patients. Fig. 3B and E shows that these two PCR products were also detected in the frontal cortex (lanes 3), the occipital cortex (lanes 4), the caudate nucleus (lanes 5), the putamen (lanes 6), the thalamus (lanes 7) and in the white matter (lanes 8), both in control subjects (Fig. 3B) and in AD patients (Fig. 3E). The total levels of PCR products showed however some variations, even taking into account the relative levels of actin mRNA by RT-PCR amplification (Figs. 2E and F, 3C and F).

3.4. *A similar profile of six tau protein isoforms is identified after dephosphorylation in the investigated brain areas*

Fig. 4 shows the pattern of soluble tau isoforms detected in the cerebellar cortex and in the temporal cortex in four control cases (Fig. 4A) and in four AD cases (Fig. 4D). Soluble tau proteins were prepared from tissue samples adjacent to those used for RNA isolation and were dephosphorylated to allow optimal separation by electrophoresis of each isoform inde-

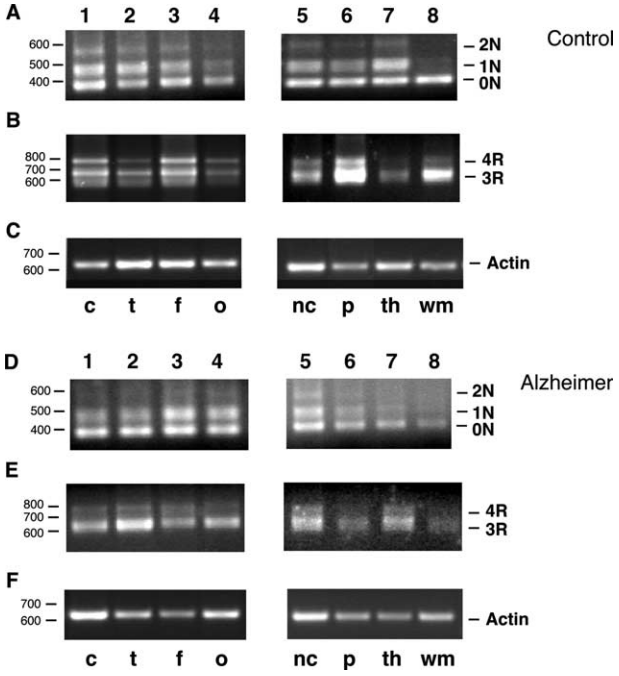

Fig. 3. Electrophoresis of RT-PCR amplification products of the 5′ domain of tau mRNAs (A and D), of the 3′ domain of tau mRNAs (B and E) and of actin mRNAs (C and F) in different brain areas in control subjects (A, B, C; lanes 1–4: case no. 4; lanes 5–8: case no. 5) and in AD patients (D, E, F; lanes 1-4: case no. 6; lanes 5–8: case no. 8). Lanes 1: cerebellar cortex (c); lanes 2: temporal cortex (t); lanes 3: frontal cortex (f); lanes 4: occipital cortex (o); lanes 5: caudate nucleus (nc); lanes 6: putamen (p); lanes 7: thalamus (th); lanes 8: white matter (wm). Numbers on the left of lanes 1 indicate the position of calibration DNA fragments (in bp).

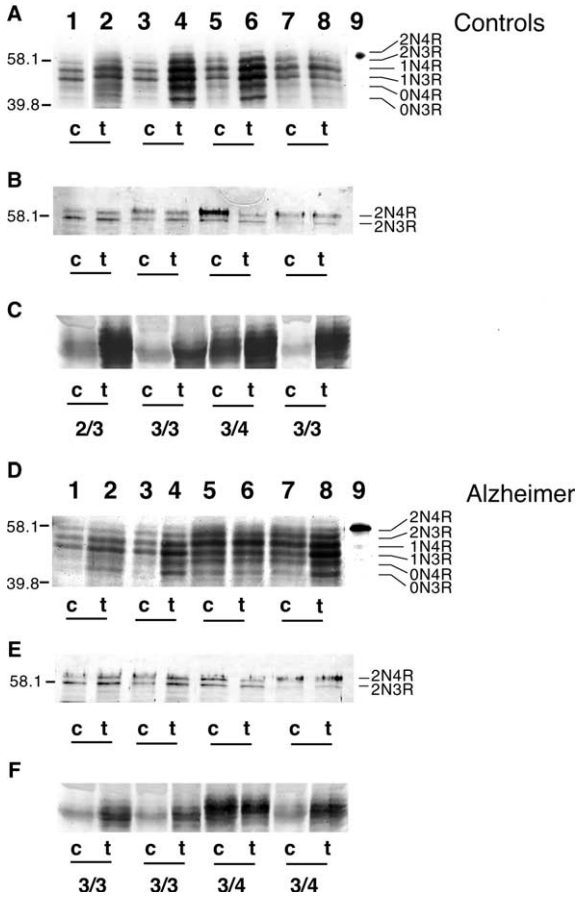

Fig. 4. Immunoblotting of soluble tau isoforms after dephosphorylation (A, B, D and E) and of total tau proteins (C and F) in the cerebellar cortex (c) and in the temporal cortex (t) in four control subjects (A–C, case nos. 2–5) and in four AD patients (D–F, case nos. 6–9). The lane 9 in A and D corresponds to the recombinant 2N4R tau protein. The blots in A, C, D and F were incubated with the B19 anti-tau antibody and the blots in B and E with the exon 3 specific anti-tau antibody (BR10). The APOE genotype of the subjects is indicated below the lines in C and F.

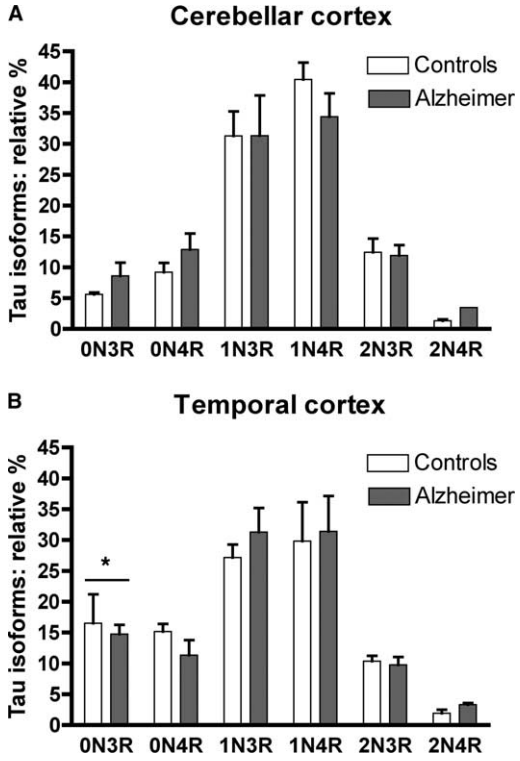

Fig. 5. Densitometry analysis of soluble tau isoform expression in the cerebellar cortex (A) and in the temporal cortex (B) in control subjects (white columns, case nos. 2–5) and in AD patients (gray columns, case nos. 6–9). Tau isoforms levels are expressed as relative percentage of the mean levels ± S.E.M. (error bars). *: $P < 0.05$ ($n = 4$, ANOVA).

pendently of its phosphorylation state. The recombinant 2N4R isoform was run in parallel to allow exact identification of the largest tau isoform extracted from tissue samples. For the sake of comparison, non-dephosphorylated total tau proteins from the same samples are shown in Fig. 4C (control cases) and in Fig. 4F (AD cases). For comparison of soluble and total tau levels in control and AD cases, the ratio between tau immunoreactivity in temporal and in cerebellar cortex (all isoforms) was calculated for each case and both for the soluble and total tau fractions. These ratios were not statistically different ($P = 0.12$, ANOVA). The six tau isoforms were identified in all soluble fractions, with the two 1N tau isoforms being the most abundant and the 2N4R and 2N3R tau isoforms being of a relatively lower abundance. The two latter tau isoforms were, however, clearly detected by the anti-exon3 tau antibody (BR10) in control cases (Fig. 4B) and in AD cases (Fig. 4E). The relative expression of each soluble tau isoform in the cerebellar cortex and in the temporal cortex was estimated by densitometry analysis in control subjects and in AD patients (Fig. 5). The relative percentage of each tau isoform was not statistically different between control subjects and AD patients. The 0N3R tau isoform was however more expressed in the temporal cortex when compared to the cerebellar cortex, both in control subjects and in AD patients (ANOVA, $P < 0.05$). The six tau isoforms were also identified in the frontal cortex (Fig. 6A and B, lanes 3), the occipital cortex (Fig. 6A and B, lanes 4), the caudate nucleus (Fig. 6A and B, lanes 5), the putamen (Fig. 6A and B, lanes 6), the thalamus (Fig. 6A and B, lanes 7), and in the white matter (Fig. 6A and

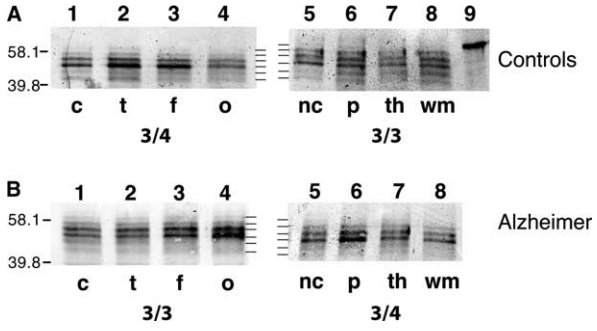

Fig. 6. Immunoblotting of soluble tau isoforms after dephosphorylation in different brain areas in control subjects (A, lanes 1–4: case no. 4; lanes 5–8: case no. 5) and in AD patients (B, lanes 1–4: case no. 6; lanes 5–8: case no. 8). Lanes 1: cerebellar cortex (c); lanes 2: temporal cortex (t); lanes 3: frontal cortex (f); lanes 4: occipital cortex (o); lanes 5: caudate nucleus (nc); lanes 6: putamen (p); lanes 7: thalamus (th); lanes 8: white matter (wm). The lane 9 in (A) corresponds to the recombinant 2N4R tau protein. The position of the tau isoforms in each blot is indicated by small bars. The APOE genotype of the subjects is indicated below the lines.

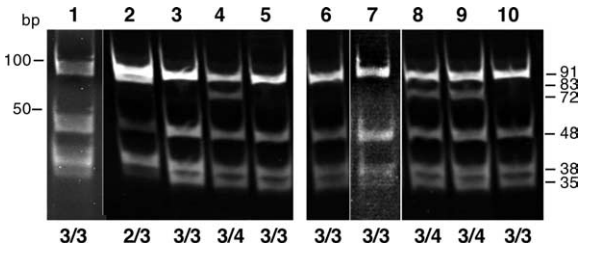

Fig. 7. ApoE genotyping of control subjects (lanes 1–5: case nos. 1–5) and AD cases (lanes 6–10: case nos. 6–10) used in this study. Lanes 1 and 7 are from different gels. PCR amplification of the APOE gene was followed by restriction isotyping. The sizes of the restriction fragments are indicated on the right and the positions of the DNA calibration fragments are indicated on the left. The APOE genotype is indicated below the lanes. As reported, the E2 allele is characterized by 91 and 83 bp fragments, the E3 allele by the 91 bp fragment and additional 48 and 35 bp fragments, and the E4 allele by the 48 and 35 bp fragments and a unique 72 bp fragment. The 38 bp fragment is common to all alleles.

B, lanes 8). This pattern was similar in control subjects (Fig. 6A) and in AD cases (Fig. 6B).

3.5. APOE genotyping in control and AD subjects

To check if the distribution of tau isoforms might be dependent on the expression of selected ApoE isoforms, the APOE genotype of all subjects was determined. Amplification of APOE gene sequences allowed the restriction isotyping of apolipoprotein E isoforms expressed in control subjects and in AD patients (Table 1 and Fig. 7). In both groups, the E3 allele was the most frequent. Two AD cases and one control subject were heterozygous for the E4 allele. The APOE genotype of subjects is indicated in Figs. 4 and 6 illustrating the tau immunoblots from different brain regions of control and AD subjects. The same tau mRNAs and the six tau isoforms were identified in the different brain regions in subjects with or without an E4 allele or other combinations of APOE alleles.

4. Discussion

Neuroanatomical variation of tau mRNAs and tau proteins expression in brain areas could underlie the propensity of selected areas to develop or not neurofibrillary lesions and this pattern might change in AD. This study was thus aimed at investigating the distribution of tau mRNA and tau protein isoforms in several neuroanatomically defined human brain areas, both in control subjects and in sporadic AD cases. The RT-PCR amplification of the 3′ domain of tau transcripts identified two products with the expected sizes for sequences containing exon 10 (4R tau mRNA) or without this exon (3R tau mRNA). The eight investigated brain areas expressed 3R and 4R tau mRNAs, consistent with previous studies [23,24]. Our study is the first one investigating in several human brain areas the pattern of expression of tau mRNA encoding different types of N-terminal inserts. The RT-PCR amplification identified three products with the expected sizes for transcripts containing exons 2 and 3, exon 2 alone, or without these exons. These three PCR products were identified in all the gray matter areas investigated. In white matter, only the short PCR product was abundantly amplified. Since glial cells are largely the most abundant cell population in the white matter, it is probable that this PCR product results from the amplification of mRNAs present in astrocytes and/or oligodendrocytes. Rodent oligodendrocytes have been reported to express tau proteins [25] and cultured rat oligodendrocytes express both 3R and 4R tau mRNA [26]. Cultured astrocytes [27] and astrocytes in situ [28] express tau proteins. In addition, astrocytic and oligodendroglial fibrillary inclusions immunoreactive for tau proteins are a common pathological feature of several tauopathies, including progressive supranuclear palsy, multiple system atrophy, and some familial forms of frontotemporal dementias [29]. Our results suggest that human glial cells in situ express mainly the 0N tau mRNAs with three or four repeats. We have, however, identified the six soluble tau protein isoforms in the white matter. This suggests that most of the tau isoforms present in the white matter are transported along axons, although some of the 0N isoforms might be synthesized in glial cells.

The neuroanatomical distribution of tau mRNAs species was similar in cortical areas prone to develop NFT (temporal and frontal cortex) and in brain areas devoid of NFT in the disease (cerebellar cortex) or less prone to develop NFT (striate occipital cortex). This might indicate that the propensity of these neocortical areas to develop NFT is not associated to a differential expression of tau mRNAs. Differential expression of tau mRNAs in cell subpopulations is nevertheless not excluded by these observations; e.g., the granule cells in the hippocampus were reported to express 3R but not 4R tau mRNAs [23]. The same tau mRNA species were expressed in controls and in AD in areas heavily affected or unaffected with NFT, suggesting that the disease is not associated to qualitative change in splicing events at the level of the tau primary transcript. In previous studies, the levels of 3R and 4R tau mRNA were not observed to be changed in the frontal cortex of AD patients [23,30], although a relative downregulation of 3R tau mRNA and an upregulation of 4R tau in areas heavily affected with NFT (e.g., temporal and frontal cortex) has been reported in one study [24].

We observed a pattern of six soluble tau isoforms in the eight brain areas investigated, with the 1N tau isoforms being systematically the most abundant, both in control and AD subjects. A previous report also indicated that the pattern of soluble tau isoforms in the frontal cortex was similar in control and AD subjects [31]. We, however, observed that the 0N3R tau isoform was significantly more abundant in the temporal cortex than in the cerebellum. Although the six tau isoforms have been identified in PHF, a relative increase in 3R tau isoforms in PHF has been reported [32,33]. The relative higher expression of 0N3R tau in the temporal cortex might thus underlie the susceptibility of this area to develop NFT. Since insoluble PHF could sequester selective tau isoforms, it is not excluded that this might have changed the relative percentage of soluble tau isoforms present in affected brain areas in AD, by comparison with controls. However, this was not reflected in the temporal cortex that showed a similar pattern of soluble tau isoforms in control and AD subjects, suggesting that either the patterns of insoluble and soluble tau isoforms are relatively similar or that a pre-existing abnormal tau pattern in AD was hidden by selective sequestration of insoluble tau leading to a similar pattern in control and AD subjects. Lastly, the relative abundance of tau proteins isoforms was apparently not reflecting the relative abundance of tau RT-PCR products (e.g., abundance of the 0N and 3R PCR products), but the absence

of quantitative RT-PCR amplifications of each tau mRNAs makes difficult direct comparisons between tau proteins isoforms and their mRNAs levels.

The E4 allele of the APOE gene has been identified as a major risk factor in familial and sporadic AD [34] and the densities of senile plaques and NFT have been reported to be higher in patients with an E4 allele [35]. We could however not distinguish a different qualitative pattern of expression of tau mRNAs or tau proteins in subjects bearing or not an E4 allele, suggesting that the susceptibility to develop NFT in ApoE4 positive patients is not directly related to a peculiar pattern of tau expression.

Altogether, our study suggests that the pattern of expression of tau mRNA transcripts and tau isoforms is not significantly changed at the topographical level in AD and that other mechanisms than a disequilibrium in the relative expression of these isoforms might be operating to foster NFT formation in sporadic cases of AD. Since our study did not investigate the changes of tau expression at the cellular level in AD, it is however still possible that changes in selective cell subpopulations might not have been detected by the present methodological approach. Although quantitative analysis of additional brain regions will be necessary, a differential expression of tau isoforms such as the one detected for the 0N3R isoform in the temporal cortex might be instrumental in the molecular mechanisms leading to NFT formation in areas susceptible to NFT formation.

Acknowledgements: This study was supported by grants from the Belgian FRSM, Alzheimer Belgique and the International Alzheimer Research Foundation.

References

[1] Buée, L., Bussière, T., Buée-Scherrer, V., Delacourte, A. and Hof, P.R. (2000) Brain Res. Rev. 33, 95–130.
[2] Avila, J., Lim, F., Moreno, F., Belmonte, C. and Cuello, A.C. (2002) Mol. Neurobiol. 25, 213–231.
[3] Goedert, M., Spillantini, M.G., Cairns, N.J. and Crowther, R.A. (1992) Neuron 8, 159–168.
[4] Brion, J.P., Hanger, D.P., Couck, A.M. and Anderton, B.H. (1991) Biochem. J. 279, 831–836.
[5] Braak, H. and Braak, E. (1991) Acta Neuropathol. (Berl.) 82, 239–259.
[6] Duyckaerts, C., Colle, M.A., Dessi, F., Grignon, Y., Piette, F. and Hauw, J.J. (1998) J. Neural. Transm. 105 (Suppl. 53), 119–126.
[7] Delacourte, A. et al. (1999) Neurology 52, 1158–1165.
[8] Tolnay, M., Sergeant, N., Ghestem, A., Chalbot, S., De Vos, R.A.I., Steur, E.N.H.J., Probst, A. and Delacourte, A. (2002) Acta Neuropathol.(Berl.) 104, 425–434.
[9] Togo, T. et al. (2002) J. Neuropathol. Exp. Neurol. 61, 547–556.
[10] Goedert, M. (2001) Curr. Opin. Genet. Dev. 11, 343–351.
[11] Lee, V.M.Y., Goedert, M. and Trojanowski, J.Q. (2001) Annu. Rev. Neurosci. 24, 1121–1159.
[12] Hutton, M. (2001) Neurology 56, S21–S25.
[13] Stanford, P.M. et al. (2003) Brain 126, 814–826.
[14] Goedert, M., Spillantini, M.G., Jakes, R., Rutherford, D. and Crowther, R.A. (1989) Neuron 3, 519–526.
[15] Kosik, K.S., Orecchio, L.D., Bakalis, S. and Neve, R.L. (1989) Neuron 2, 1389–1397.
[16] Hixson, J.E. and Vernier, D.T. (1990) J. Lipid Res. 31, 545–548.
[17] Hanger, D.P., Gibb, G.M., de Silva, R., Boutajangout, A., Brion, J.P., Revesz, T., Lees, A.J. and Anderton, B.H. (2002) FEBS Lett. 531, 538–542.
[18] Brion, J.P., Hanger, D.P., Bruce, M.T., Couck, A.M., Flament-Durand, J. and Anderton, B.H. (1991) Biochem. J. 273, 127–133.
[19] Brion, J.P., Tremp, G. and Octave, J.N. (1999) Am. J. Pathol. 154, 255–270.
[20] Mulot, S.F.C., Hughes, K., Woodgett, J.R., Anderton, B.H. and Hanger, D.P. (1994) FEBS Lett. 349, 359–364.
[21] Guillemette, J.G., Wong, L., Crapper McLachlan, D.R. and Lewis, P.N. (1986) J. Neurochem. 47, 987–997.
[22] Preece, P. and Cairns, N.J. (2003) Mol. Brain Res. 118, 60–71.
[23] Goedert, M., Spillantini, M.G., Potier, M.C., Ulrich, J. and Crowther, R.A. (1989) EMBO J. 8, 393–399.
[24] Yasojima, K., McGeer, E.G. and McGeer, P.L. (1999) Brain Res. 831, 301–305.
[25] LoPresti, P., Szuchet, S., Papasozomenos, S.C., Zinkowski, R.P. and Binder, L.I. (1995) Proc. Natl. Acad. Sci. USA 92, 10369–10373.
[26] Müller, R., Heinrich, M., Heck, S., Blohm, D. and Richter-Landsberg, C. (1997) Cell Tissue Res. 288, 239–249.
[27] Couchie, D., Fages, C., Bridoux, A.M., Rolland, B., Tardy, M. and Nunez, J. (1985) J. Cell Biol. 101, 2095–2103.
[28] Papasozomenos, S.C. (1989) Lab. Invest. 60, 123–137.
[29] Richter-Landsberg, C. (2000) J. Neurosci. Res. 59, 11–18.
[30] Chambers, C.B., Lee, J.M., Troncoso, J.C., Reich, S. and Muma, N.A. (1999) Ann. Neurol. 46, 325–332.
[31] Goedert, M. and Jakes, R. (1990) EMBO J. 9, 4225–4230.
[32] Greenberg, S.G., Davies, P., Schein, J.D. and Binder, L.I. (1992) J. Biol. Chem. 267, 564–569.
[33] Ksiezak-Reding, H., Shafit-Zagardo, B. and Yen, S.-H. (1995) J. Neurosci. Res. 41, 583–593.
[34] Saunders, A.M. et al. (1993) Neurology 43, 1467–1472.
[35] Yamada, T., Kondo, A., Takamatsu, J., Tateishi, J. and Goto, I. (1995) J. Neurol. Sci. 129, 56–61.